Article

Direct NMR Detection of Alkali Metal Ions Bound to G-Quadruplex DNA

Ramsey Ida, and Gang Wu

J. Am. Chem. Soc., **2008**, 130 (11), 3590-3602 • DOI: 10.1021/ja709975z

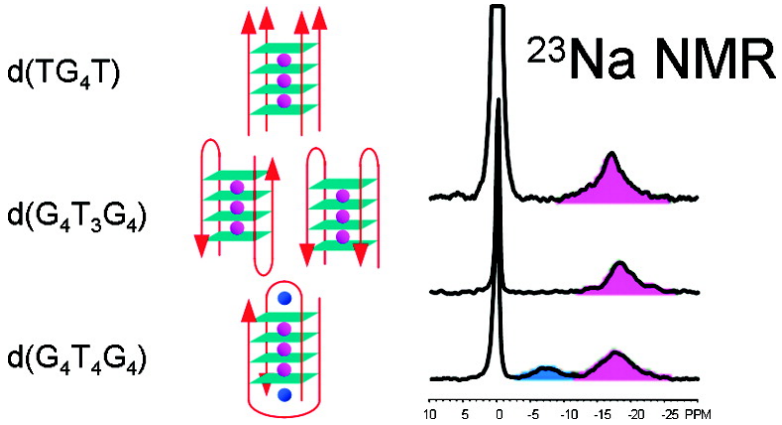

More About This Article

Additional resources and features associated with this article are available within the HTML version:

- Supporting Information
- Links to the 8 articles that cite this article, as of the time of this article download
- Access to high resolution figures
- Links to articles and content related to this article
- Copyright permission to reproduce figures and/or text from this article

View the Full Text HTML

J|A|C|S
ARTICLES
Published on Web 02/23/2008

Direct NMR Detection of Alkali Metal Ions Bound to G-Quadruplex DNA

Ramsey Ida and Gang Wu*

Department of Chemistry, Queen's University, 90 Bader Lane, Kingston, Ontario, Canada K7L 3N6

Received November 5, 2007; E-mail: gang.wu@chem.queensu.ca

Abstract: We describe a general multinuclear (^{1}H, ^{23}Na, ^{87}Rb) NMR approach for direct detection of alkali metal ions bound to G-quadruplex DNA. This study is motivated by our recent discovery that alkali metal ions (Na^+, K^+, Rb^+) tightly bound to G-quadruplex DNA are actually "NMR visible" in solution (Wong, A.; Ida, R.; Wu, G. *Biochem. Biophys. Res. Commun.* **2005**, *337*, 363). Here solution and solid-state NMR methods are developed for studying ion binding to the classic G-quadruplex structures formed by three DNA oligomers: $d(TG_4T)$, $d(G_4T_3G_4)$, and $d(G_4T_4G_4)$. The present study yields the following major findings. (1) Alkali metal ions tightly bound to G-quadruplex DNA can be directly observed by NMR in solution. (2) Competitive ion binding to the G-quadruplex channel site can be directly monitored by simultaneous NMR detection of the two competing ions. (3) Na^+ ions are found to locate in the diagonal T_4 loop region of the G-quadruplex formed by two strands of $d(G_4T_4G_4)$. This is the first time that direct NMR evidence has been found for alkali metal ion binding to the diagonal T_4 loop in solution. We propose that the loop Na^+ ion is located above the terminal G-quartet, coordinating to four guanine O6 atoms from the terminal G-quartet and one O2 atom from a loop thymine base and one water molecule. This Na^+ ion coordination is supported by quantum chemical calculations on ^{23}Na chemical shifts. Variable-temperature ^{23}Na NMR results have revealed that the channel and loop Na^+ ions in $d(G_4T_4G_4)$ exhibit very different ion mobilities. The loop Na^+ ions have a residence lifetime of 220 μs at 15 °C, whereas the residence lifetime of Na^+ ions residing inside the G-quadruplex channel is 2 orders of magnitude longer. (4) We have found direct ^{23}Na NMR evidence that mixed K^+ and Na^+ ions occupy the $d(G_4T_4G_4)$ G-quadruplex channel when both Na^+ and K^+ ions are present in solution. (5) The high spectral resolution observed in this study is unprecedented in solution ^{23}Na NMR studies of biological macromolecules. Our results strongly suggest that multinuclear NMR is a viable technique for studying ion binding to G-quadruplex DNA.

Introduction

Alkali metal ions such as Na^+ and K^+ are known to play important roles in the formation, stability, and structural polymorphism of G-quadruplex DNA and RNA.[1−9] Although a large number of G-quadruplexes have been structurally characterized by either solution NMR spectroscopy or crystallography, detailed information regarding the mode of alkali metal ion binding in G-quadruplex DNA and RNA has become available only recently from high-resolution crystallographic studies.[10−25] Meanwhile, solid-state NMR has also emerged in the past several years as a new method for directly detecting alkali metal ions in G-quadruplex DNA and related systems.[26−36] Compared to crystallography and solid-state NMR techniques,

(1) Guschlbauer, W.; Chantot, J. F.; Thiele, D. *J. Biomol. Struct. Dyn.* **1990**, *8*, 491−511.
(2) Sen, D.; Gilbert, W. *Methods Enzymol.* **1992**, *211*, 191−199.
(3) Williamson, J. R. *Annu. Rev. Biophys. Biomol. Struct.* **1994**, *23*, 703−730.
(4) Gilbert, D. E.; Feigon, J. *Curr. Opin. Struct. Biol.* **1999**, *9*, 305−314.
(5) Keniry, M. A. *Biopolymers* **2000**, *56*, 123−146.
(6) Neidle, S.; Parkinson, G. N. *Curr. Opin. Struct. Biol.* **2003**, *13*, 275−283.
(7) Davis, J. T. *Angew. Chem., Int. Ed.* **2004**, *43*, 668−698.
(8) Burge, S.; Parkinson, G.; Hazel, P.; Todd, A. K.; Neidle, S. *Nucleic Acids Res.* **2006**, *34*, 5402−5415.
(9) Neidle, S.; Balasubramanian, S. *Quadruplex Nucleic Acids*; The Royal Society of Chemistry: Cambridge, U.K., 2006.
(10) Kang, C.; Zhang, X. H.; Ratliff, R.; Moyzis, R.; Rich, A. *Nature* **1992**, *356*, 126−131.
(11) Laughlan, G.; Murchie, A. I. H.; Norman, D. G.; Moore, M. H.; Moody, P. C. E.; Lilley, D. M. J.; Luisi, B. *Science* **1994**, *265*, 520−524.
(12) Phillips, K.; Dauter, Z.; Murchie, A. I. H.; Lilley, D. M. J.; Luisi, B. *J. Mol. Biol.* **1997**, *273*, 171−182.
(13) Horvath, M. P.; Schultz, S. C. *J. Mol. Biol.* **2001**, *310*, 367−377.
(14) Deng, J. P.; Xiong, Y.; Sundaralingam, M. *Proc. Natl. Acad. Sci. U.S.A.* **2001**, *98*, 13665−13670.
(15) Parkinson, G. N.; Lee, M. P. H.; Neidle, S. *Nature* **2002**, *417*, 876−880.
(16) Haider, S.; Parkinson, G. N.; Neidle, S. *J. Mol. Biol.* **2002**, *320*, 189−200.
(17) Clark, G. R.; Pytel, P. D.; Squire, C. J.; Neidle, S. *J. Am. Chem. Soc* **2003**, *125*, 4066−4067.
(18) Haider, S. M.; Parkinson, G. N.; Neidle, S. *J. Mol. Biol.* **2003**, *326*, 117−125.
(19) Pan, B.; Xiong, Y.; Shi, K.; Deng, J.; Sundaralingam, M. *Structure* **2003**, *11*, 815−823.
(20) Pan, B. C.; Xiong, Y.; Shi, K.; Sundaralingam, M. *Structure* **2003**, *11*, 825−831.
(21) Caceres, C.; Wright, G.; Gouyette, C.; Parkinson, G.; Subirana, J. A. *Nucleic Acids Res.* **2004**, *32*, 1097−1102.
(22) Kondo, J.; Adachi, W.; Umeda, S.; Sunami, T.; Takenaka, A. *Nucleic Acids Res.* **2004**, *32*, 2541−2549.
(23) Hazel, P.; Parkinson, G. N.; Neidle, S. *J. Am. Chem. Soc.* **2006**, *128*, 5480−5487.
(24) Gill, M. L.; Strobel, S. A.; Loria, J. P. *Nucleic Acids Res.* **2006**, *34*, 4506−4514.
(25) Lee, M. P. H.; Parkinson, G. N.; Hazel, P.; Neidle, S. *J. Am. Chem. Soc.* **2007**, *129*, 10106−10107.
(26) Wu, G. *Biochem. Cell Biol.* **1998**, *76*, 429−442.
(27) Rovnyak, D.; Baldus, M.; Wu, G.; Hud, N. V.; Feigon, J.; Griffin, R. G. *J. Am. Chem. Soc.* **2000**, *122*, 11423−11429.
(28) Wu, G.; Wong, A. *Chem. Commun.* **2001**, 2658−2659.

10.1021/ja709975z CCC: $40.75

it is much more difficult to study alkali metal ion binding to G-quadruplex DNA in solution. In the early studies for self-assembly of 5′-guanosine monophosphate, Laszlo and co-workers[37−39] used solution ^{23}Na, ^{39}K, and ^{87}Rb NMR results to establish the first model for ion binding to a G-quartet structure. Later, Braunlin and co-workers[40,41] attempted to use solution ^{23}Na and ^{39}K NMR techniques to directly study ion binding to G-quadruplex DNA. However, their conclusion was that alkali metal ions tightly bound to a G-quadruplex DNA are "invisible" to NMR in solution, because of low signal intensity and unfavorable quadrupole spin relaxation properties. As a result, they utilized an indirect approach where NMR relaxation properties of alkali metal ions are measured for the averaged signal and analyzed using either two-site or three-site chemical exchange models. From such a relaxation data analysis, one can only infer ion binding information for the tightly bound sites.

Since the late 1990s, NMR methodologies based on spin-$^1/_2$ probes such as ^{15}N and ^{205}Tl have been developed by Feigon and co-workers[42−44] and by Strobel and co-workers[45,46] for directly probing NH_4^+ and Tl^+ ions in G-quadruplex DNA. Recently, Plavec and co-workers[47−50] have used this approach to gain a tremendous amount of new information about NH_4^+ ion movement inside G-quadruplex channels.

In 2005, we discovered that, in contrast to the conclusion drawn by Barunlin and co-workers, alkali metal ions (Na^+, K^+, and Rb^+) tightly bound to a G-quadruplex structure can be directly observed by ^{23}Na, ^{39}K, and ^{87}Rb NMR even in the liquid state.[51] This immediately opens the door for directly studying alkali metal ion binding to G-quadruplex DNA. Here we apply this new multinuclear NMR methodology to examine alkali metal ion binding to the classic G-quadruplex structures formed by three DNA oligomers: d(TG_4T), d($G_4T_3G_4$), and d($G_4T_4G_4$).

The G-quadruplex structure formed by DNA hexamer d(TG_4T) in the presence of Na^+ ions has been characterized by both solution NMR[52,53] and X-ray crystallography.[11,12] In solution, four d(TG_4T) strands form a parallel-stranded G-quadruplex structure containing four stacked G-quartets. This structure was also shown to maintain in solution when Na^+ ions are replaced by K^+ ions. The crystal structures of the Na^+ form of d(TG_4T) showed a four-stranded parallel structure similar to the solution structure. Interestingly, the crystal structure of d(TG_4T) also revealed a distinct intermolecular stacking not mentioned in the solution NMR studies. This intermolecular stacking consists of a pair of quadruplex structures that are stacked at the 5′ ends. In the high-resolution crystal structure, a total of seven Na^+ ions are located either between or within the G-quartet planes. Solid-state ^{23}Na NMR has confirmed that Na^+ ions between two adjacent G-quartets in d(TG_4T) give rise to a ^{23}Na NMR signal centered at −19 ppm;[27,29] however, the signal from the in-plane Na^+ ions has been illusive because of the presence of a large signal due to phosphate-bound Na^+ ions. In solution, only one ^{23}Na NMR signal at −17 ppm was observed for Na^+ ions tightly bound to d(TG_4T),[51] raising the question whether the mode of Na^+ ion binding is the same in solution and solid states. In a recent study, Clark et al.[17] published a crystal structure of d(TG_4T) complexed to a drug molecule, daunomycin. This crystal structure shows that daunomycin prefers to be stacked onto the ends of the G-quadruplex rather than to intercalate between the G-quartet layers. It is interesting to note that, in this crystal structure, Na^+ ions are located only between adjacent G-quartet planes.

The crystal structures of the K^+ form of d($G_4T_3G_4$) have been reported by Neidle and co-workers.[23] d($G_4T_3G_4$) forms a bimolecular intermolecular G-quadruplex with two lateral thymine loops. The two lateral T_3 loops could be either on the same G-quadruplex face, forming a head-to-head dimer, or on the opposite faces, resulting in a head-to-tail dimer. K^+ ions were found between G-quartets, each being equidistant from eight O6 guanine atoms. This crystallographic study also suggests that there are not large energy differences between the head-to-head and head-to-tail bimolecular G-quadruplexes containing the T_3 loops and that both of these forms may be present in solution.

The bimolecular G-quadruplex structure formed by d($G_4T_4G_4$) has been extensively characterized by solution NMR and crystallographic studies.[13,16,18,54−56] This DNA oligomer is related to the repeat sequence d(T_4G_4) found in the *Oxytricha nova* telomere. In solution, d($G_4T_4G_4$) generally adopts an antiparallel, bimolecular quadruplex structure consisting of four stacked G-quartets and two diagonal thymine loops. Feigon and co-workers examined the structural details between various ionic forms of d($G_4T_4G_4$) in solution and concluded that the nature of monovalent cations present in the solution (Na^+, K^+ and

(29) Wong, A.; Fettinger, J. C.; Forman, S. L.; Davis, J. T.; Wu, G. *J. Am. Chem. Soc.* **2002**, *124*, 742−743.
(30) Wu, G.; Wong, A.; Gan, Z. H.; Davis, J. T. *J. Am. Chem. Soc.* **2003**, *125*, 7182−7183.
(31) Wong, A.; Wu, G. *J. Am. Chem. Soc.* **2003**, *125*, 13895−13905.
(32) Wu, G.; Wong, A. *Biochem. Biophys. Res. Commun.* **2004**, *323*, 1139−1144.
(33) Ida, R.; Wu, G. *Chem. Commun.* **2005**, 4294−4296.
(34) Wu, G.; Wong, A. Solid-state nuclear magnetic resonance studies of alkali metal ions in nucleic acids and related systems. In *NMR Spectroscopy of Biological Solids*; Ramamoorthy, A., Ed.; CRC Press: Boca Raton, FL, 2006; pp 317−344.
(35) Zhong, C.; Wang, J.; Wu, N.; Wu, G.; Zavalij, P. Y.; Shi, X. *Chem. Commun.* **2007**, 3148−3150.
(36) Kwan, I. C. M.; Mo, X.; Wu, G. *J. Am. Chem. Soc.* **2007**, *129*, 2398−2407.
(37) Delville, A.; Detellier, C.; Laszlo, P. *J. Magn. Reson.* **1979**, *34*, 301−315.
(38) Borzo, M.; Detellier, C.; Laszlo, P.; Paris, A. *J. Am. Chem. Soc.* **1980**, *102*, 1124−1134.
(39) Detellier, C.; Laszlo, P. *J. Am. Chem. Soc.* **1980**, *102*, 1135−1141.
(40) Xu, Q. W.; Deng, H.; Braunlin, W. H. *Biochemistry* **1993**, *32*, 13130−13137.
(41) Deng, H.; Braunlin, W. H. *J. Mol. Biol.* **1996**, *255*, 476−483.
(42) Hud, N. V.; Schultze, P.; Feigon, J. *J. Am. Chem. Soc.* **1998**, *120*, 6403−6404.
(43) Hud, N. V.; Schultze, P.; Sklenar, V.; Feigon, J. *J. Mol. Biol.* **1999**, *285*, 233−243.
(44) Feigon, J.; Butcher, S. E.; Finger, L. D.; Hud, N. V. *Methods Enzymol.* **2001**, *338*, 400−420.
(45) Basu, S.; Szewczak, A. A.; Cocco, M.; Strobel, S. A. *J. Am. Chem. Soc.* **2000**, *122*, 3240−3241.
(46) Gill, M. L.; Strobel, S. A.; Loria, J. P. *J. Am. Chem. Soc* **2005**, *127*, 16723−16732.
(47) Sket, P.; Crnugelj, M.; Kozminski, W.; Plavec, J. *Org. Biomol. Chem.* **2004**, *2*, 1970−1973.
(48) Sket, P.; Crnugelj, M.; Plavec, J. *Nucleic Acids Res.* **2005**, *33*, 3691−3697.
(49) Sket, P.; Plavec, J. *J. Am. Chem. Soc.* **2007**, *129*, 8794−8800.
(50) Podbevsek, P.; Hud, N. V.; Plavec, J. *Nucleic Acids Res.* **2007**, *35*, 2554−2563.
(51) Wong, A.; Ida, R.; Wu, G. *Biochem. Biophys. Res. Commun.* **2005**, *337*, 363−366.
(52) Aboul-ela, F.; Murchie, A. I. H.; Lilley, D. M. J. *Nature* **1992**, *360*, 280−282.
(53) Aboul-ela, F.; Murchie, A. I. H.; Norman, D. G.; Lilley, D. M. J. *J. Mol. Biol.* **1994**, *243*, 458−471.
(54) Smith, F. W.; Feigon, J. *Nature* **1992**, *356*, 164−168.
(55) Hud, N. V.; Smith, F. W.; Anet, F. A. L.; Feigon, J. *Biochemistry* **1996**, *35*, 15383−15390.
(56) Schultze, P.; Hud, N. V.; Smith, F. W.; Feigon, J. *Nucleic Acids Res.* **1999**, *27*, 3018−3028.

NH_4^+) does not affect the overall fold of d($G_4T_4G_4$).[56] In the presence of Ca^{2+}, however, d($G_4T_4G_4$) can undergo a structural transition from an antiparallel to a parallel quadruplex, which in turn can aggregate into a large molecular assembly known as the G-wire.[57]

The crystal structure of the K^+ form of d($G_4T_4G_4$) (PDB entries 1JRN, 1JPQ) showed that the overall quadruplex structure of d($G_4T_4G_4$) in the solid state is very similar to that found in solution.[16] Moreover, the crystal structures yielded explicit information about the mode of ion binding in d($G_4T_4G_4$). In particular, three K^+ ions are found to reside inside the quadruplex channel, each being sandwiched between two adjacent G-quartets. Two additional K^+ ions are observed in the thymine loop regions. The Tl^+ form of d($G_4T_4G_4$) (PDB entry 2HBN)[24] exhibits essentially the same structure as the K^+ form. Interestingly, when an acridine derivative interacts with d($G_4T_4G_4$), the drug molecule enters into one of the thymine loop regions, replacing the loop K^+ ion in the same loop but leaving the other loop K^+ ion unperturbed.[18] In the crystal structure for the Na^+ form of a d($G_4T_4G_4$)-protein complex (PDB entry 1JB7), a completely different mode of ion binding was observed by Horvath and Schultz.[13] They found that two Na^+ ions are located nearly coplanar with the two central G-quartets, and two additional Na^+ ions are located in the thymine loop regions. Although these crystallographic studies have provided unequivocal evidence about the mode of K^+, Tl^+, and Na^+ ion binding both inside the quadruplex channel and in the thymine loop region, it is far less certain whether the same type of ion binding should occur in solution for the Na^+ form of d($G_4T_4G_4$). For the NH_4^+ form of d($G_4T_4G_4$), Feigon and co-workers[43] found that three NH_4^+ ions are located inside the G-quadruplex channel in a way identical to the mode of K^+ binding observed in the crystal structure. However, no NMR evidence was found for NH_4^+ ions to be located in the thymine loop region. In our solid-state ^{23}Na NMR study of d($G_4T_4G_4$), we established that three Na^+ ions reside inside the G-quadruplex channel, each being sandwiched between two adjacent G-quartets.[32] This is clearly different from the mode of Na^+ ion binding observed for the channel Na^+ ions in the crystal structure of a d($G_4T_4G_4$)−protein complex.[13] In a recent solution ^{205}Tl NMR study of d($G_4T_4G_4$), Gill et al.[46] identified the four signals between 80 and 150 ppm as due to Tl^+ ions bound to the bimolecular G-quadruplex structure formed by d($G_4T_4G_4$). Two of the four ^{205}Tl NMR signals were assigned to the Tl^+ ions inside the quadruplex channel in the same coordination environment as those seen for K^+, NH_4^+, and Na^+, and the other two signals were attributed to the Tl^+ ions residing in the thymine loop region. Despite these crystallographic and NMR studies, the question regarding the exact mode of Na^+ ion binding in d($G_4T_4G_4$) has remained unanswered.

In this study, we have chosen to examine the G-quadruplex structures formed by d(TG_4T), d($G_4T_3G_4$), and d($G_4T_4G_4$) for the following reasons. First, the G-quadruplex structures formed from these DNA oligomers have been fully characterized by either solution NMR or crystallography. Second, they represent three classic types of G-quadruplexes: parallel-stranded, bimolecular with lateral loops, and bimolecular with diagonal loops. Third, no information is available regarding the mode of Na^+ ion binding to these G-quadruplexes in solution.

Experimental Details

Sample Preparation. DNA oligonucleotides of d(TG_4T), d($G_4T_3G_4$), and d($G_4T_4G_4$) were synthesized by Cortec DNA Service Laboratories, Inc. (Kingston, ON, Canada) and by Sigma-Genosys Canada (Oakville, ON, Canada). All DNA oligomers were purified by reverse-phase cartridges. The Na^+ forms of DNA oligomers were prepared by dissolving each purified DNA oligonucleotide in 1 mL of deionized water followed by extensive dialysis against 250, 50, and 1 mM NaCl(aq). A microdialyzer and cellulose dialysis membranes with molecular weight cutoff of 500 Da (Sigma-Aldrich) and 1000 Da (Sialomed, Inc.) were used in all dialysis experiments. The DNA oligomers were then lyophilized using a freeze-dryer (Labconco Freezone 4.5) operating at $(480 \pm 5) \times 10^{-3}$ mbar and 324 ± 1 K. For NMR experiments, DNA oligomers were dissolved in sodium phosphate buffer (pH 7.1, in either H_2O:D_2O 4:1 or 100% D_2O) with appropriate amounts of NaCl added. To obtain the strand concentrations of the DNA solutions, we used a Varian Cary 100 Bio UV−vis spectrometer and the following A_{260} extinction coefficients (ϵ): d(TG_4T), 57 800; d($G_4T_3G_4$), 107 100; d($G_4T_4G_4$), 121 200. The total Na^+ ion concentration, $[Na^+]_{total}$, in each DNA sample was also measured experimentally using an external NaCl(aq) standard and ^{23}Na NMR experiments.

NMR Experiments. All solution multinuclear NMR spectra were recorded on Bruker Avance-400 (9.4 T), Avance-500 (11.7 T), and Avance-600 (14.1 T) NMR spectrometers. For ^{1}H NMR experiments, the WATERGATE sequence was employed to suppress the water signal.[58] For the WATERGATE sequence, the delays for the homogradient pulse, the binomial water suppression, and the homospoil gradient pulse were set to 200 μs, 86 μs, and 1 ms, respectively. For ^{1}H DOSY experiments, the pulse sequence of longitudinal eddy current delay (LED) with bipolar-gradient pulses was used.[59] The pulse field gradient duration varied from 2.6 to 2.8 ms, and the variable gradient strength was changed from 6 to 350 mT·m^{-1}. The diffusion period was varied from 60 to 100 ms. A total of 32 transients were collected for each of the 8 increment steps, with a recycle delay of 30 s and 64K complex points. The eddy current delay was set to 5 μs. For solution ^{23}Na NMR experiments, a 5-mm quartz NMR tube (NE-HQ5-7, New Era Enterprises, Inc.) was used to reduce the ^{23}Na background signal from regular glass materials. The 1D ^{23}Na NMR spectra were acquired using an inversion−recovery sequence with the interpulse delay (recovery delay) set to appropriate values depending on the actual T_1 value for the free ^{23}Na signal. The ^{23}Na NMR spectra were obtained with 2048 complex points and a spectral window of 35 kHz. The radio frequency (rf) field strength at the ^{23}Na Larmor frequency was 16 kHz. All ^{23}Na chemical shifts were referenced to an external NaCl(aq) sample, $\delta(^{23}\text{Na}) = 0$ ppm. Other experimental details for DNA samples are given in the figure captions. Various NaCl(aq) standard samples were also prepared for measuring very small concentrations of Na^+ ions in DNA samples. It is important to point out that, because these NaCl(aq) standard samples have much longer ^{23}Na spin−lattice relaxation times (T_1) than the DNA samples, ^{23}Na NMR spectra of standard samples must be obtained under the full relaxation recovery condition in order to obtain quantitative spectral information. For example, $T_1(^{23}\text{Na})$ is 60 ms at 298 K for a solution of 56 mM NaCl(aq). All 1D ^{87}Rb NMR spectra were obtained using the single-pulse sequence and a spectral window of 160 kHz. The ^{87}Rb spin−lattice relaxation times are much shorter than those of ^{23}Na nuclei. All ^{87}Rb chemical shifts were referenced to an external RbCl(aq) sample, $\delta(^{87}\text{Rb}) = 0$ ppm. Solid-state ^{23}Na NMR spectra were obtained on a Bruker Avance-II 900 (21.1 T) spectrometer using a 4-mm magic angle

(57) Miyoshi, D.; Nakao, A.; Sugimoto, N. *Nucleic Acids Res.* **2003**, *31*, 1156−1163.
(58) Piotto, M.; Saudek, V.; Sklenar, V. *J. Biomol. NMR* **1992**, *2*, 661−665.
(59) Wu, D. H.; Chen, A.; Johnson, C. S. *J. Magn. Reson. Ser. A* **1995**, *115*, 260−264.

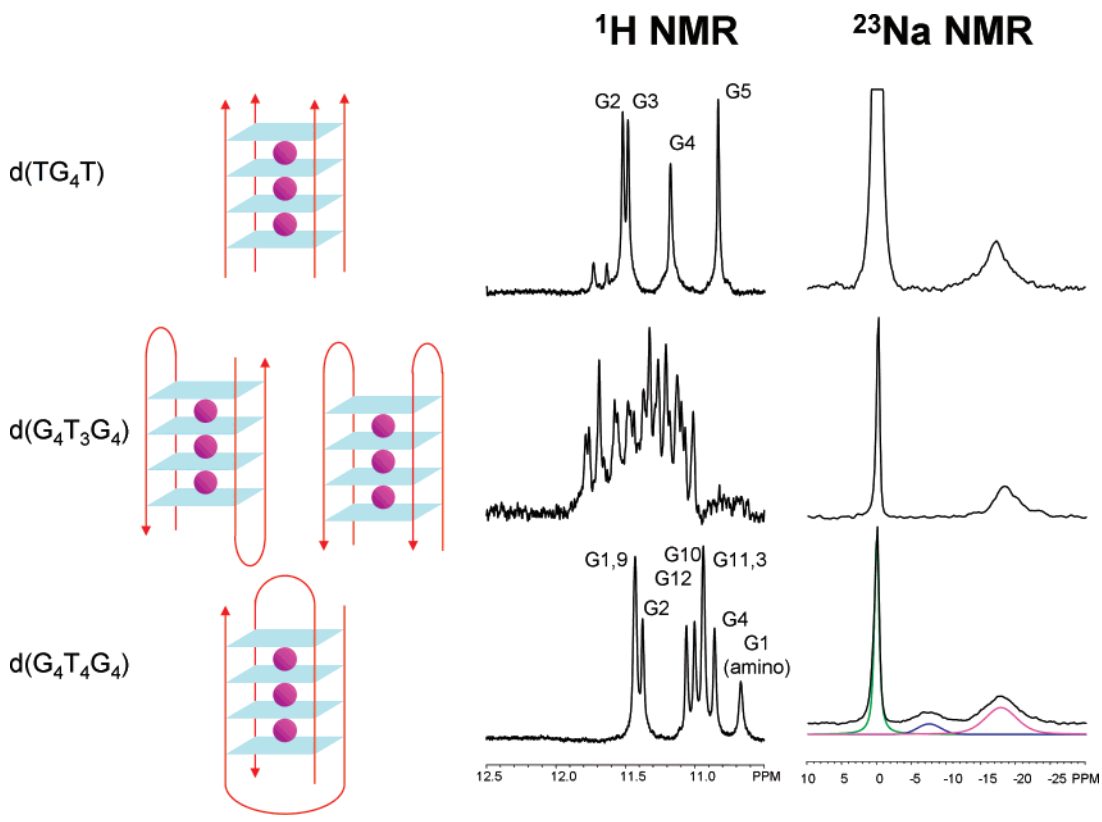

Figure 1. Schematic diagrams showing the folded G-quadruplex structures (left), spectral regions for imino protons of the ^{1}H NMR spectra (middle), and ^{23}Na NMR spectra (right) of d(TG$_4$T), d(G$_4$T$_3$G$_4$), and d(G$_4$T$_4$G$_4$). All ^{1}H and ^{23}Na NMR spectra were obtained at 278 K on a Bruker Avance-600 spectrometer (14.1 T) operating at 600.13 and 158.76 MHz for ^{1}H and ^{23}Na nuclei, respectively. DNA sample concentrations and ^{23}Na NMR experimental parameters are given below. d(TG$_4$T): 8.0 mM strand concentration; $[Na^+]_{total}$ = 140 mM; interpulse delay = 13.0 ms; 248 886 transients; recycle delay, 20 ms. d(G$_4$T$_3$G$_4$): 2.5 mM strand concentration; $[Na^+]_{total}$ = 76 mM, interpulse delay = 11.2 ms; 386 699 transients; recycle delay, 0 ms. d(G$_4$T$_4$G$_4$): 5.4 mM strand concentration; $[Na^+]_{total}$ = 70 mM; interpulse delay = 5.3 ms; 713 561 transients; recycle delay, 20 ms.

spinning (MAS) probe. The sample spinning frequency was 10 kHz. During data acquisition, ^{1}H decoupling of 100 kHz was applied. The solid DNA sample (ca. 3 mg) was packed into a 4-mm ZrO_2 rotor with a Teflon spacer and then equilibrated in a closed container with a saturated solution of NH_4Cl for 2 days, which leads to a relative humidity of ca. 80% for the DNA sample. This turned out to be important for obtaining high-quality ^{23}Na MAS spectra for solid DNA samples. With an airtight rotor cap, the DNA sample inside the rotor can maintain its relative humidity for several weeks, even after sample spinning at 10 kHz for days.

Quantum Chemical Computations. Quantum chemical calculations were performed using the Gaussian 03 (G03) suite of programs[60] on a SunFire 25000 symmetric multiprocessor system. Each of the four nodes is equipped with 24 × 1.05 GHz (8 MB E-Cache) UltraSPARC-III processor and 96 GB of RAM. Positions of hydrogen atoms were added using standard bond distances: C−H, 1.08 Å; N−H, 1.01 Å; and O−H, 0.96 Å. For Na atoms, a triple-ξ correlation consistent basis set, cc-pVTZ, was used, and a 3-21G(d) basis set was used for all other atoms. Shielding calculations were performed at the Hartree−Fock (HF) level using the gauge-independent atomic orbital (GIAO) method as implemented in G03. The computed absolute isotropic shielding constant (σ_{iso}) was converted to the chemical shift (δ_{iso}) scale using $\delta_{iso} = \sigma_{ref} - \sigma_{iso}$, where σ_{ref} is the absolute shielding constant for the reference sample, Na^+(aq). At the HF/3-21G(d)/cc-pVTZ level, we found σ_{ref} to be 587.7 ppm for $[Na(H_2O)_6]^+$, whose geometry was fully optimized at MP2/6-311++G** ($Na-O_W$ = 2.433 Å). All computations were performed at the High Performance Computing Virtual Laboratory (HPCVL) of Queen's University.

Results and Discussion

Direct Observation of Na^+ Ions inside the G-Quadruplex Channel. Figure 1 shows ^{1}H and ^{23}Na NMR spectra for the Na^+ forms of d(TG$_4$T), d(G$_4$T$_3$G$_4$), and d(G$_4$T$_4$G$_4$). The observed imino ^{1}H NMR signals for d(TG$_4$T) and d(G$_4$T$_4$G$_4$) are in excellent agreement with those reported previously,[61] confirming the formation of fully folded G-quadruplex structures in our DNA samples. For d(G$_4$T$_3$G$_4$), no solution ^{1}H NMR structure has been reported in the literature. However, the sharp imino ^{1}H NMR signals observed for d(G$_4$T$_3$G$_4$) (shown in Figure 1) are characteristic of G-quadruplex structures. The large number of imino ^{1}H NMR signals (ca. 16 peaks) suggests that either d(G$_4$T$_3$G$_4$) forms an asymmetric dimeric G-quadruplex or two dimeric G-quadruplex structures coexist in solution. As mentioned earlier, the crystallographic study of the K^+ form of d(G$_4$T$_3$G$_4$) indeed suggests that head-to-tail antiparallel and head-to-head dimers are both possible.[23] A similar situation was reported in the G-quadruplex structures formed by d(TG$_4$T$_2$G$_4$T).[62]

Before we discuss ^{23}Na NMR results, a general concern regarding ^{23}Na NMR studies of DNA is worth commenting. Because the concentration of free Na^+ ions often greatly exceeds the concentration of DNA, it is necessary to employ NMR techniques to suppress the large ^{23}Na NMR signal arising from free Na^+ ions, allowing much weaker signals due to DNA-bound Na^+ ions to be effectively detected. In this study we used an

(60) Frisch, M. J.; et al. *Gaussian 03*, Revision C.02; Gaussian, Inc.: Wallingford, CT, 2004.
(61) Smith, F. W.; Feigon, J. *Biochemistry* **1993**, *32*, 8682−8692.
(62) Phan, A. T.; Modi, Y. S.; Patel, D. J. *J. Mol. Biol.* **2004**, *338*, 93−102.

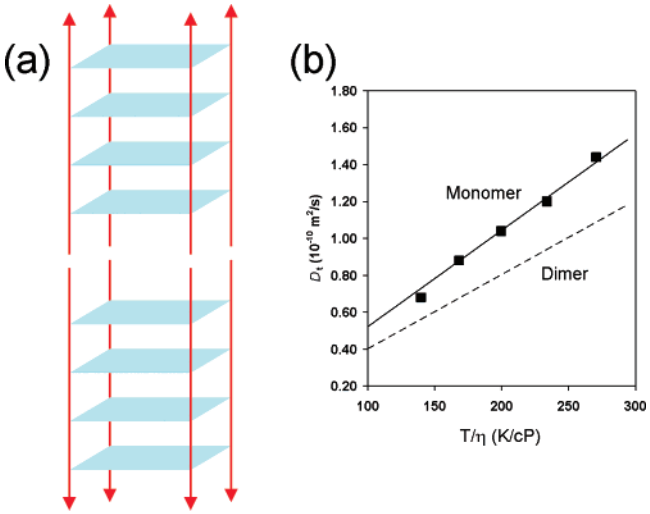

Figure 2. (a) Illustration of the dimer formation of d(TG$_4$T) G-quadruplex in the solid state. (b) Stokes−Einstein plot of the diffusion data measured for d(TG$_4$T) in D$_2$O.

inversion−recovery pulse sequence to suppress the large signal from the free Na^+ ions ($\delta = 0$ ppm). It should be emphasized that the ^{23}Na NMR signal at $\delta = 0$ ppm (denoted as the free Na^+ signal) is actually the averaged signal for Na^+ ions undergoing fast exchange between a truly free state and a phosphate-bound state. Because the free Na^+ ions have a much longer spin−lattice relaxation time (typically $T_1 \approx 10$ ms) than do the tightly bound Na^+ ions (typically $T_1 < 1$ ms), we can set the interpulse delay (recovery delay) to be very close to the so-called null (zero-crossing) point for the free Na^+ ions so that the signal from the free Na^+ ions would be greatly reduced, whereas the signals from the bound Na^+ ions have already fully recovered at this point and thus show their full intensities in the spectra. In this regard, the inversion−recovery sequence works as a T_1 filter. We have found this method to be very effective in obtaining high-quality ^{23}Na NMR spectra for DNA.

As seen in Figure 1, one common spectral feature in the ^{23}Na NMR spectra of d(TG$_4$T), d(G$_4$T$_3$G$_4$), and d(G$_4$T$_4$G$_4$) is that a well-defined signal is observed at −17.7 ppm. Our previous studies have established unambiguously that this signal is due to Na^+ ions residing inside the G-quadruplex channel, each Na^+ ion being coordinated to eight O6 guanine atoms.[29] To assess the Na^+ ion occupancy inside the G-quadruplex channel, we determined the concentration of Na^+ ions that give rise to the ^{23}Na NMR signal at −17.7 ppm in each of the three DNA samples: d(TG$_4$T), 5.6 ± 0.8 mM; d(G$_4$T$_3$G$_4$), 3.5 ± 0.8 mM; and d(G$_4$T$_4$G$_4$), 7.6 ± 0.8 mM. For d(G$_4$T$_3$G$_4$) and d(G$_4$T$_4$G$_4$), it is straightforward to estimate the ion occupancy, because each bimolecular G-quadruplex has three channel sites. Thus, the maximum Na^+ ion occupancy inside the channel for 2.5 mM d(G$_4$T$_3$G$_4$) and 5.4 mM d(G$_4$T$_4$G$_4$) is 3.7 and 8.1 mM, respectively. Comparing these values with the experimental data, we can conclude that the Na^+ ion occupancy inside the G-quadruplex channel formed by d(G$_4$T$_3$G$_4$) and d(G$_4$T$_4$G$_4$) is approximately 100%. That is, each G-quadruplex channel contains three Na^+ ions. For d(TG$_4$T), the situation is slightly complicated, because there is a possibility for d(TG$_4$T) to form two stacking tetramolecular G-quadruplexes, as suggested by the crystal structures of d(TG$_4$T),[11] as illustrated in Figure 2. Because the two stacking G-quadruplexes are related by symmetry, it is not possible to assess this dimer formation simply

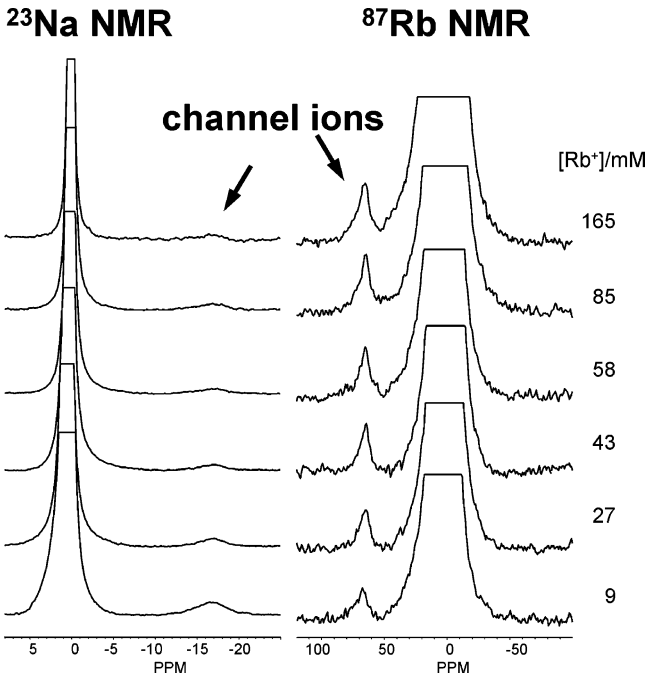

Figure 3. Experimental results from a Rb^+/Na^+ titration experiment for d(TG$_4$T). (Left) ^{23}Na NMR spectra obtained using the inversion−recovery sequence. (Right) ^{87}Rb NMR spectra obtained using the single-pulse excitation sequence and identical conditions (628 206 transients and 10 ms recycle delay). All NMR spectra were recorded on a Bruker Avance-600 (14.1 T) spectrometer at 298 K. The initial DNA sample was prepared at 3 mM strand concentration in 30 mM sodium phosphate buffer (pH 7.1).

from ^{1}H NMR spectra. For this purpose, we used ^{1}H DOSY NMR to determine the molecular translational coefficient (D) of the d(TG$_4$T) G-quadruplex. We found that $D = 1.44$, 1.20, 1.04, 0.88 and (0.68 ± 0.04) × 10^{-10} m^2/s at 298, 293, 288, 283, and 278 K, respectively. Using a combined bead/cylinder model developed in our previous study,[63] we estimate the length of the d(TG$_4$T) G-quadruplex to be 20 ± 4 Å in D$_2$O, which is roughly half of the length for the G-quadruplex dimer found in the crystal structures. The DOSY results shown in Figure 2 provide unambiguous evidence that d(TG$_4$T) does not form a dimer of G-quadruplexes in solution at the DNA concentrations used in our study. Once we are certain about the G-quadruplex structure of d(TG$_4$T) in solution, we can estimate the Na^+ ion occupancy inside the channel. Similar to the situations discussed earlier for d(G$_4$T$_3$G$_4$) and d(G$_4$T$_4$G$_4$), we found that the three channel sites inside the d(TG$_4$T) G-quadruplex channel are fully occupied by three Na^+ ions. This immediately suggests that the mode of Na^+ ion binding (particularly the existence of in-plane Na^+ ions) observed in the crystal structures may be due to a crystal packing effect. Of course, our NMR data cannot completely rule out the possibility that in-plane Na^+ binding may also occur, but on a much shorter time scale.

The fact that the ^{23}Na NMR signal for channel Na^+ ions is well separated from that for free Na^+ ions immediately suggests that the chemical exchange between these two types of Na^+ ions must be slow on the ^{23}Na chemical shift NMR time scale. In fact, we have observed similar ^{23}Na NMR spectra for these DNA oligomers at a lower magnetic field, 9.4 T. At 9.4 T, a 17 ppm separation between the channel and free Na^+ ions corresponds to a frequency separation of approximately 1800

(63) Wong, A.; Ida, R.; Spindler, L.; Wu, G. *J. Am. Chem. Soc.* **2005**, *127*, 6990−6998.

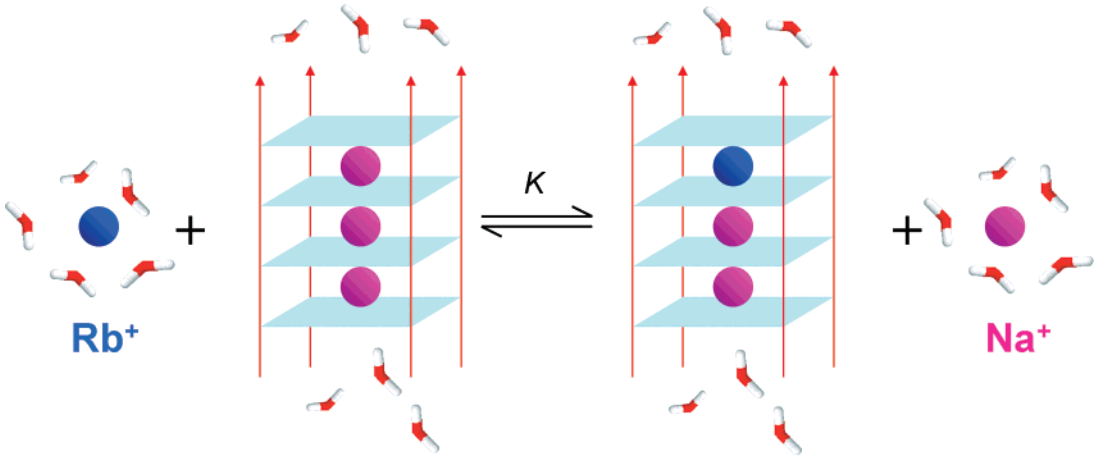

Figure 4. Illustration of the competitive Rb^+/Na^+ ion binding for the channel site of d(TG_4T) G-quadruplex.

Hz. Therefore, the residence time for Na^+ ions inside the G-quadruplex channel must be much longer than $1/(1800 \times 2\pi)$ Hz = 90 μs at 298 K (*vide infra*).

Competitive Binding of Na^+ and Rb^+ Ions for the G-Quadruplex Channel Site. Because now we can observe well-defined NMR signals for alkali metal ions residing inside the G-quadrupelx channel, it becomes possible to study competitive ion binding by simultaneously detecting the two competing metal ions. Here we use d(TG_4T) as an example to illustrate this application. Figure 3 show the results of a Rb^+/Na^+ titration experiment where various amounts of Rb^+ ions are added to the Na^+ form of d(TG_4T). In each of the ^{87}Rb NMR spectra, two signals are observed, at 0 and 70 ppm. The signal at 0 ppm arises from Rb^+ ions undergoing fast exchange between free and phosphate-bound states. The signal at 70 ppm is due to Rb^+ ions residing inside the G-quadruplex channel. This observed ^{87}Rb chemical shift is in excellent agreement with our previously established ^{87}Rb NMR signature for channel Rb^+ ions.[33] Both signals exhibit a single Lorentzian line shape, suggesting that both types of Rb^+ ions in d(TG_4T) are in the regime of $\omega_0\tau_C < 1$. This is quite different from the case of Rb^+ binding to 5′-GMP self-assembly in solution.[51] The ^{87}Rb NMR results shown in Figure 3 represent the first time that a distinct ^{87}Rb NMR signal is observed for Rb^+ ions tightly bound to any DNA. It is also clearly seen from Figure 3 that, when Rb^+ ions are added to the DNA, they gradually replace the Na^+ ions that have previously occupied the channel site inside the G-quadruplex. This process is illustrated in Figure 4.

In aqueous solution, Rb^+ and Na^+ ions compete for the G-quadruplex channel site, and the equilibrium process can be described as

$$\underset{\text{channel ion}}{G_4{-}Na^+{-}G_4} + \underset{\text{free ion}}{Rb^+(aq)} \overset{K}{\rightleftharpoons} \underset{\text{channel ion}}{G_4{-}Rb^+{-}G_4} + \underset{\text{free ion}}{Na^+(aq)} \quad (1)$$

where the equilibrium constant (K) is defined as

$$K = \frac{[Rb^+]_{channel}[Na^+]_{free}}{[Rb^+]_{free}[Na^+]_{channel}} \quad (2)$$

In our Rb^+/Na^+ titration experiment, we add only Rb^+ ions to the DNA solution where both $[Na^+]_{total}$ and [DNA] are known. We also have $[Na^+]_{channel} + [Rb+]_{channel} = [DNA] \times$ 3/4, assuming full ion occupancy inside the channel (i.e., 3 ions in $[d(TG_4T)]_4$) and no DNA unfolding during the Rb^+/Na^+ titration experiment. Indeed ^{1}H NMR data confirmed that the d(TG_4T) G-quadruplex remained fully folded during the Rb^+/Na^+ titration experiment. Under such circumstances, one can readily show that the Rb^+ ions residing inside the channel can be expressed as

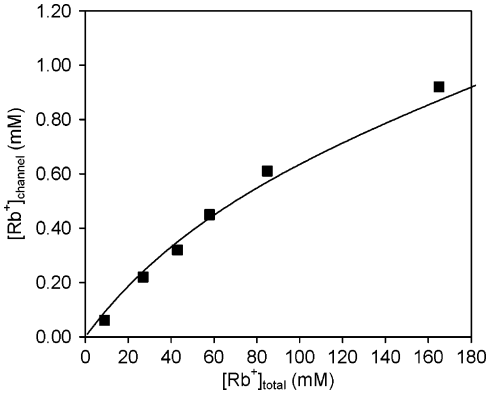

Figure 5. Comparison between experimental and calculated data from Rb^+/Na^+ titration experiments for d(TG_4T).

$$[Rb^+]_{channel} = \frac{b - \sqrt{b^2 - 4(K-1)K[G_4][Rb^+]_{total}}}{2(K-1)} \quad (3)$$

where

$$b = [Na^+]_{total} + K[Rb^+]_{total} + (K-1)[G_4] \quad (4)$$

In the Rb^+/Na^+ titration experiments, because $[Rb^+]_{total}$, $[Na^+]_{total}$, and $[G_4]$ are known, one can use eq 3 to fit the curve of $[Rb^+]_{channel}$ versus $[Rb^+]_{total}$, to obtain the value of K. It should be noted that, in our Rb^+/Na^+ titration experiments, because we added aliquots of Rb^+ stock solutions to the DNA sample, $[Na^+]_{total}$ was not constant. Rather, $[Na^+]_{total}$ decreases as a function of the added Rb^+ in the following fashion:

$$[Na^+]_{total} = [Na^+]_{initial} - 0.004[Rb^+]_{total} \quad (5)$$

Combining eqs 3−5, we were able to fit the experimental data as shown in Figure 5. The data analysis yields $K = 1.6 \pm 0.2$ at 298 K for the Rb^+/Na^+ competition for the G-quadruplex channel site. This suggests that Rb^+ ions are preferred over Na^+

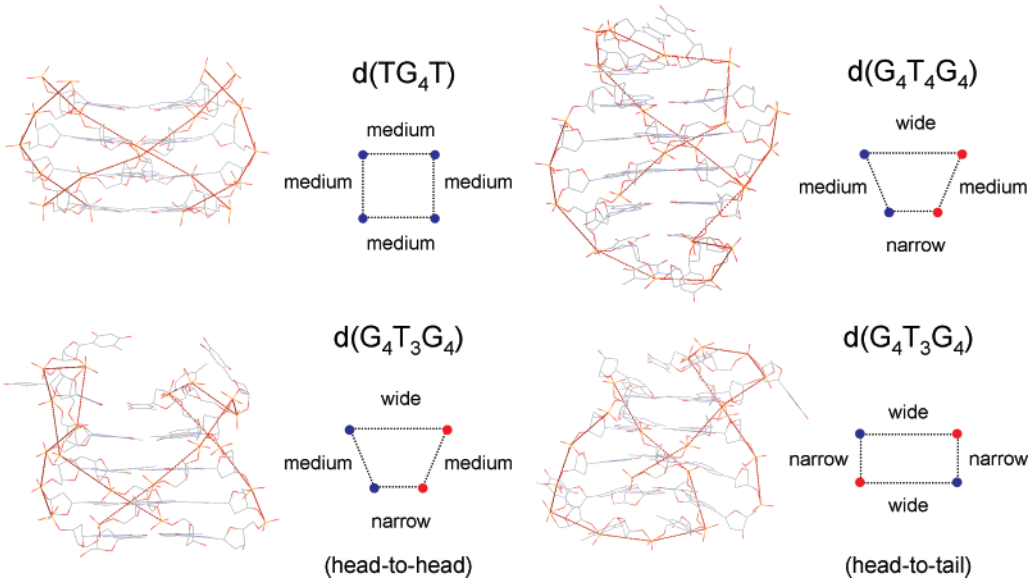

Figure 6. Illustration of groove formation in the G-quadruplex structures formed by d(TG$_4$T), d(G$_4$T$_4$G$_4$), and d(G$_4$T$_3$G$_4$). The dotted line connects the phosphate backbone to highlight the origin of groove formation. The blue and red circles indicate *anti* and *syn* glycosidic conformation, respectively.

by the channel site of the G-quadruplex channel, in agreement with the known affinity sequence for G-quadruplex DNA.[7] This value of K is also in agreement with that reported by Wong and Wu[31] for 5′-GMP, $K \approx 1.8$ at 298 K, on the basis of a solid-state NMR titration experiment. Our new solution NMR data thus prove that the solid-state NMR method for determining Rb^+/Na^+ binding affinity is a valid approach for obtaining solution properties. This is not surprising, because the Na^+ ion at the channel site is fully dehydrated, so there should be no difference as to whether this Rb^+/Na^+ competition is measured in solution or in the solid state. In a recent study of 5′-GMP, we observed two separate ^{23}Na NMR signals, at −17.0 and −16.2 ppm, for channel Na^+ ions.[64] The former signal corresponds to the Na^+ ions inside a G-quadruplex filled with Na^+ ions, while the latter is due to Na^+ ions in a channel containing mixed Rb^+/Na^+ ions. The same process should occur in d(TG$_4$T) during the Rb^+/Na^+ titration experiment. However, because the channel Na^+ ion signal for d(TG$_4$T) is much broader than that found for 5′-GMP (500 Hz in DNA versus 284 Hz in 5′-GMP at 278 K), we did not observe resolved ^{23}Na NMR signals for the channel Na^+ ions. However, as will be shown later in this study, the situation is different in the K^+/Na^+ titration experiment.

Similar to the earlier discussion about the residence time of Na^+ ions inside the channel, the frequency separation between the two ^{87}Rb NMR signals (9.2 kHz at 9.4 T) also allows us to conclude that the residence time of Rb^+ ions inside the G-quadruplex channel must be much longer than 17 μs at 298 K. Recently, Halle and co-workers[65] demonstrated a magnetic relaxation dispersion (MRD) NMR approach to study competitive Rb^+ and Na^+ binding to the minor groove of a *B*-DNA duplex, [d(CGCGAATTCGCG)]$_2$. In this case, the ion binding is relatively weak, and the mean residence time is 0.2 μs for Rb^+ ions and 10 ns to 100 μs for Na^+ ions. These values are much shorter than those estimated for the Na^+ and Rb^+ ions residing inside a G-quadruplex channel. As a result, only an averaged NMR signal was observed by Halle and co-workers in ^{23}Na and ^{87}Rb NMR spectra of the *B*-DNA duplex. Clearly, a combination of our direct NMR observation method and the MRD approach should allow one to examine competitive ion binding to DNA on a wide range of time scales.

Observation of Na^+ Ions in the T$_4$ Loop Region of d(G$_4$T$_4$G$_4$). Figure 1 also shows that, in addition to the signal from channel Na^+ ions, the ^{23}Na NMR spectrum of d(G$_4$T$_4$G$_4$) exhibits another signal, at −7.4 ppm. Our hypothesis is that this signal is due to Na^+ ions in the thymine loop regions (referred to as the loop Na^+ ions in this study). In this section, we provide evidence to support this assignment. For a general G-quadruplex structure, there are four regions where ion binding may potentially occur: phosphate, groove, loop, and channel. In our previous study[51] and from the results presented in the previous section, we have established the ^{23}Na NMR spectral characteristics for phosphate-bound and channel Na^+ ions. Here we discuss the other two possible regions for ion binding. Figure 6 illustrates the groove regions in the G-quadruplexes formed by d(TG$_4$T), d(G$_4$T$_3$G$_4$), and d(G$_4$T$_4$G$_4$). In the parallel-stranded G-quadruplex of d(TG$_4$T), all glycosidic bonds of the guanine bases are in *anti* conformation, resulting in the formation of four equally wide groove regions. If we use the closest distance between two phosphate oxygen atoms across the groove to define groove width, the width of the groove in d(TG$_4$T) is in a range between 8.30 and 9.53 Å (see Table 1), which can be considered as a medium groove. For the dimeric G-quadruplex formed by d(G$_4$T$_4$G$_4$), the pattern in glycosidic torsion angles within each G-quartet is *syn*−*syn*−*anti*−*anti*; together with the diagonal topology, this generates three groove regions: one narrow groove (6.76 Å), two medium grooves (10.59 and 10.26 Å), and one wide groove (14.74 Å). For the dimeric G-quadruplexes formed by d(G$_4$T$_3$G$_4$), while the head-to-tail dimer has two alternating grooves, narrow (7.64 and 7.69 Å) and wide (16.64 and 16.03 Å), the head-to-head dimer exhibits one narrow groove (6.55 Å), two medium grooves (10.29 and 10.21 Å), and one wide groove (14.17 Å). As seen from Table 1, the grooves found in the head-to-head dimer of d(G$_4$T$_3$G$_4$) have

(64) Ida, R.; Kwan, I. C. M.; Wu, G. *Chem. Commun.* **2007**, 795−797.
(65) Marincola, F. C.; Denisov, V. P.; Halle, B. *J. Am. Chem. Soc.* **2004**, *126*, 6739−6750.

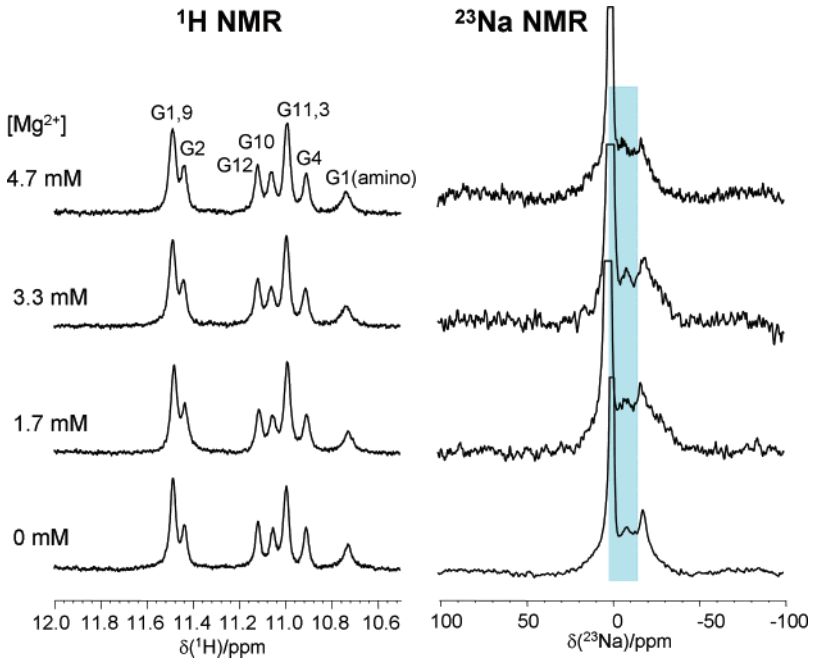

Figure 7. (Left) ^{1}H and (right) ^{23}Na NMR spectra of d($G_4T_4G_4$) (1.3 mM strand concentration and $[Na^+]_{total}$ = 41 mM) in a Mg^{2+} ion titration experiment. All NMR spectra were obtained at 281 K on a Bruker Avance-500 (11.7 T) spectrometer.

Table 1. Summary of the Shortest Distances between Phosphorus Atoms in Groove Regions of G-Quadruplex DNA

		shortest P–P distances (Å) in groove regions		
DNA	PDB entry	narrow	medium	wide
d(TG_4T)	244D		9.53 9.25 8.30 8.64	
d($G_4T_4G_4$)	1JPQ	6.76	10.59 10.26	14.74
d($G_4T_3G_4$) (head-to-head)	2AJV	6.55	10.29 10.21	14.17
d($G_4T_3G_4$) (head-to-tail)	2AVH	7.69 7.64		16.64 16.03

essentially the same widths as those observed in d($G_4T_4G_4$). In general, when a narrow groove is present, it is possible for cross-phosphate ion binding to occur. However, essentially the same types of narrow grooves are present in both d($G_4T_4G_4$) and d($G_4T_3G_4$), but the ^{23}Na NMR signal at −7.4 ppm is observed only in d($G_4T_4G_4$). This observation should rule out the possibility that this signal is due to Na^+ ions tightly bound to the narrow groove regions crossing two phosphate groups. Therefore, we conclude that this signal is most likely to arise from Na^+ ions residing in the diagonal T_4 loop regions.

To further confirm this assignment, we performed another titration experiment where Mg^{2+} ions were added to the Na^+ form of d($G_4T_4G_4$). It is well known that the divalent Mg^{2+} ions interact more strongly with the DNA phosphates but do not enter the G-quadrupelx channel. As seen from Figure 7, both of the ^{23}Na NMR signals at −7.4 and −17.7 ppm remain unchanged when Mg^{2+} ions are added to the DNA solution. On the other hand, the line width of the ^{23}Na signal at 0 ppm, which arises from Na^+ ions undergoing fast exchange between free and phosphate-bound states, decreases from 190 Hz before the titration experiment to 46 Hz when the concentration of Mg^{2+} ions reaches 4.7 mM. This drastic line-width reduction suggests that Mg^{2+} ions compete very effectively only for the DNA phosphate backbone. In contrast, as will be discussed later, K^+ ions are capable of competing for all three sites.

Modeling the Na^+ Ion Binding Site in the T_4 Loop. Several years ago, Feigon and co-workers[56] proposed a model to describe the mode of Na^+ binding in the Na^+ form of d($G_4T_4G_4$). They suggested that, while one Na^+ ion is sandwiched between the two central G-quartets, each of the two outer Na^+ ions lies in the terminal G-quartet plane, coordinating to four O6(G) atoms and one O2(T) atom in a penta-coordination geometry. Recently, they also used this model to interpret the observed trend in trans-H-bond scalar couplings, $^{2h}J_{N2N7}$.[66] However, the subtle structural differences between different ionic forms of d($G_4T_4G_4$), inferred from the observed $^{2h}J_{N2N7}$ values, do not necessarily lead to the conclusion that the cation binding site must be different. In contradiction to this model, both solid-state ^{23}Na NMR results[32] and the new solution ^{23}Na NMR data presented in this study show that there are already three Na^+ ions residing inside the G-quadruplex channel of d($G_4T_4G_4$), each being sandwiched between two adjacent G-quartet planes. Then it is not possible for another Na^+ ion to reside within the terminal G-quartet plane, because the Na^+−Na^+ repulsion would be too great. One of the rationales that Feigon and co-workers used to propose a penta-coordination environment for the terminal Na^+ ion is the close proximity (ca. 3.6 Å) between the O2 atom from thymine 7 (T7) and the geometrical center of the terminal G-quartet, suggested by the solution NMR structure of the Na^+ form of d($G_4T_4G_4$) (PDB entry 156D).[56,67] However, if a Na^+ ion were to reside within the terminal G-quartet plane, this distance would be too long for Na^+−O coordination. Close inspection of the aforementioned solution NMR structure reveals that the O2 atom from T7 does not lie directly above the geometrical center of the terminal G-quartet,

(66) Dingley, A. J.; Peterson, R. D.; Grzesiek, S.; Feigon, J. *J. Am. Chem. Soc.* **2005**, *127*, 14466−14472.
(67) Schultze, P.; Smith, F. W.; Feigon, J. *Structure* **1994**, *2*, 221−233.

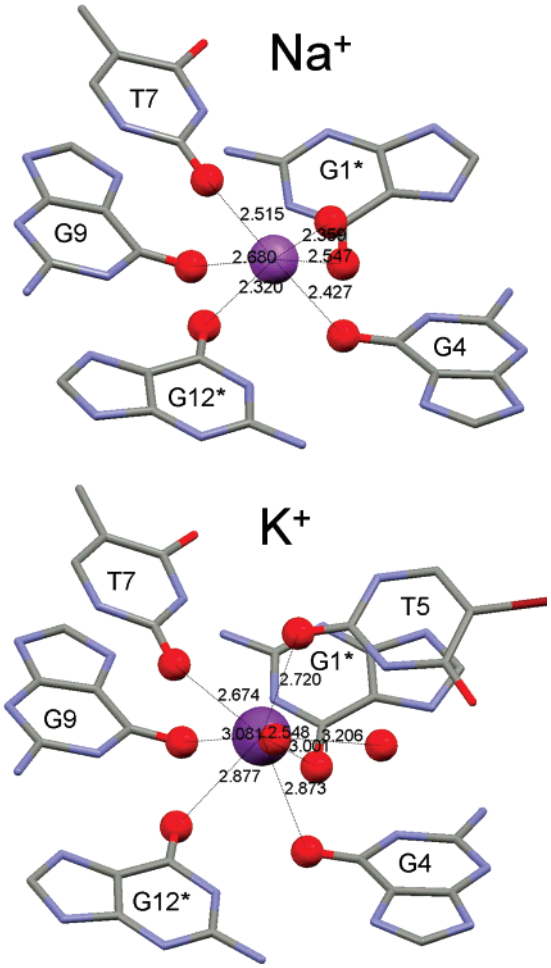

Figure 8. (Top) Molecular model of the Na^+ ion binding site in the T_4 loop of $d(G_4T_4G_4)$. (Bottom) Crystal structure of the K^+ ion binding site in the T_4 loop of $d(G_4T_4G_4)$ (PDB entries 1JRN and 1JPQ). The symmetry-related residues are marked by asterisks.

as required for a square pyramidal coordination geometry. Instead, the O2(T7) atom is located nearly directly above the O6(G9) atom, considerably off the central axis of the quadruplex channel.

On the basis of currently available information about ^{23}Na chemical shifts in organic Na salts,[34] the observed ^{23}Na chemical shift for the loop Na^+ ions in $d(G_4T_4G_4)$, −7.4 ppm, suggests that the Na^+ ion in the T_4 loop region is most likely to have a hexa-coordination geometry. Here we propose that the loop Na^+ ion in $d(G_4T_4G_4)$ lies above the terminal G-quartet plane, coordinating to the four O6 atoms from G9, G1*, G4, and G12*, the O2 atom from T7, and a water molecule in a hexa-coordination geometry. Because we had recently shown that *ab initio* ^{23}Na chemical shift calculations for G-quartet systems can yield very accurate results,[64] we decided to apply this computational approach to help interpret the observed ^{23}Na chemical shift in terms of an exact Na^+ coordination geometry in the T_4 loop. For this purpose, we constructed a model using the structural information from the solution NMR structure of the Na^+ form of $d(G_4T_4G_4)$ (PDB entry 156D) and the crystal structure of a $d(G_4T_4G_4)$/protein complex (PDB entry 1JB7). As shown in Figure 8, the model consists of a terminal G-quartet, a thymine base (T7), a water molecule, and a Na^+ ion (a total of 81 atoms). The water molecule is likely hydrogen-bonded to the O2 atom from T5 (not shown in Figure 8), because

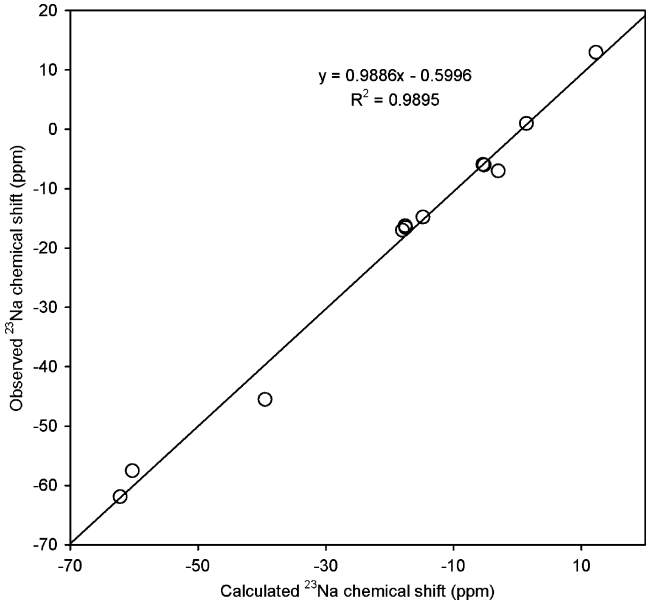

Figure 9. Correlation between experimental and calculated ^{23}Na chemical shifts for selected organic systems.

the O_W−O2(T5) distance is approximately 2.74 Å, well within the hydrogen-bond distance range. For comparison, we also show in Figure 8 the structural details about the K^+ ion in the same T_4 loop of $d(G_4T_4G_4)$, which were determined by crystallography (PDB entries 1JRN and 1JPQ).[16]

The computed ^{23}Na chemical shift at the HF/3-21G(d)/cc-pVTZ level for the model shown in Figure 8 is −3 ppm. Considering the approximations used in the model construction, this calculated ^{23}Na chemical shift is in reasonable agreement with the observed value, −7.4 ppm. To assess the accuracy of quantum chemical calculations, we show in Figure 9 a comparison between experimental and computed ^{23}Na chemical shifts for a range of organic Na^+ complexes including crown ethers,[68] G-quartets,[64] cation−π systems,[69,70] and metallocenes.[71] The experimental data from these systems cover essentially the entire ^{23}Na chemical shift range. As seen in Figure 9, quantum chemical computations at the restricted Hartree−Fock level with triple-ξ basis sets can yield quite reliable results for ^{23}Na chemical shifts. Thus, quantum chemical calculations provide additional confirmation for our hypothesis regarding the Na^+ ion coordination in the T_4 loop.

Solid-State ^{23}Na NMR Spectra of $d(G_4T_4G_4)$. Now we have established that Na^+ ions are located in the T_4 loop region of $d(G_4T_4G_4)$ in solution. However, why did we not observe this signal in the solid-state ^{23}Na NMR spectra of $d(G_4T_4G_4)$ in a previous study?[32] Close inspection of those solid-state ^{23}Na NMR spectra reveals that this loop signal, if present, is likely to be obscured by the broad signal arising from phosphate-bound Na^+ ions. To provide a definite answer to the question of whether the loop Na^+ ions can be observed in the solid-state ^{23}Na NMR spectra, we decided to re-examine this problem. We prepared a new solid $d(G_4T_4G_4)$ sample with the following modifications in sample preparation. First, we did not perform

(68) Tossell, J. A. *J. Phys. Chem. B* **2001**, *105*, 11060−11066.
(69) Wong, A.; Whitehead, R. D.; Gan, Z. H.; Wu, G. *J. Phys. Chem. A* **2004**, *108*, 10551−10559.
(70) Bryce, D. L.; Adiga, S.; Elliott, E. K.; Gokel, G. W. *J. Phys. Chem. A* **2006**, *110*, 13568−13577.
(71) Willans, M. J.; Schurko, R. W. *J. Phys. Chem. B* **2003**, *107*, 5144−5161.

dialysis of the DNA sample against Cs^+ ions as we did in our previous study, so the d($G_4T_4G_4$) sample is in the pure Na^+ form, identical to the one studied by solution NMR discussed earlier in this study. Second, we prepared the solid DNA sample under a constant relative humidity, ca. 80% (see Experimental Details). In addition, we performed the solid-state ^{23}Na NMR experiment at 21.1 T (900 MHz for ^1H) to increase the chemical shift dispersion between different signals. As shown in Figure 10a, the signal from the phosphate-bound Na^+ ions in the ^{23}Na MAS spectrum of d($G_4T_4G_4$) becomes much narrower than that in the previous study (i.e., 650 Hz in the new DNA sample versus 1600 Hz in a dry DNA). However, it is still difficult to see whether there is any additional weak signal around −7 ppm. Here, we further utilized a rotor-synchronized spin echo experiment to selectively suppress the phosphate-bound Na^+ ions because they have a shorter T_2 than the other signals. As a result, the T_2-filtered ^{23}Na MAS spectrum shown in Figure 10b,c clearly shows a signal centered at −8 ppm, in addition to the channel Na^+ signal centered at −17 ppm. It should be noted that the peak position (δ_{obs}) in the solid-state ^{23}Na MAS NMR spectra does not correspond to the true isotropic chemical shift (δ_{iso}). It is well known that these two quantities are related by[72]

$$\delta_{obs} = \delta_{iso} - \frac{10^6}{120}\left(\frac{C_Q}{\nu_0}\right)^2(3 + \eta_Q{}^2) \quad \text{[ppm]} \qquad (6)$$

where C_Q is the nuclear quadrupole coupling constant, η_Q is the asymmetry parameter, and ν_0 is the Larmor frequency of the ^{23}Na nuclei. Using the ^{23}Na quadrupole parameters reported in our previous study for d($G_4T_4G_4$) (C_Q = 0.9−1.2 MHz, η_Q = 0.4−1.0),[32] we estimate that the correction due to the second term in eq 6 is on the order of 0.4−0.8 ppm at 21.1 T (ν_0 = 238.1 MHz for ^{23}Na). Thus, the ^{23}Na chemical shifts for both loop and channel Na^+ ions measured from the solid-state NMR spectra are in excellent agreement with those found in solution. Furthermore, the fact that both types of solid-state ^{23}Na NMR signals have similar line widths is also consistent with the solution ^{23}Na NMR spectra. We can now conclude that the loop Na^+ ions in d($G_4T_4G_4$) are present in both solution and solid states.

Na^+ Ions in the T_4 Loop Are Less Tightly Bound Than the Channel Ions. In this section, we return to discuss more ^{23}Na NMR results for d($G_4T_4G_4$) in solution. Figure 11 shows the ^{23}Na NMR spectra of d($G_4T_4G_4$) obtained at different temperatures. At 5 °C, the line widths for the loop and channel Na^+ ions are 620 and 855 Hz, respectively. As the temperature is increased, the signal from the loop Na^+ ions becomes considerably broadened (ca. 950 Hz at 10 °C), decreases in its total area, and disappears completely at temperatures ≥15 °C. In contrast, the line width for the channel Na^+ signal changes only 6% for the entire temperature range from 5 to 25 °C. This immediately suggests that the loop Na^+ ions are less tightly bound (or more mobile) than the channel Na^+ ions, and thus they undergo a much faster exchange between the bound and free states. As seen from Figure 11, if we take 15 °C as the coalescence temperature for an asymmetrical chemical exchange process between the loop binding and free states, a chemical-exchange line shape analysis with p_A/p_B = 0.07/0.93 and a chemical shift difference of 1174 Hz (7.4 ppm at 158.7 MHz for ^{23}Na) yields a residence lifetime (τ_R) of 0.22 ± 0.03 ms for the loop Na^+ ion in the bound state; thus, $k_{off} \approx 1/\tau_R = 4.5 \times 10^3\ s^{-1}$ at 15 °C. If we assume that the observed line width for the loop Na^+ ion signal is completely due to exchange broadening, the same line shape analysis yields 0.4 and 0.3 ms for the Na^+ residence lifetime at 5 and 10 °C, respectively. These residence lifetimes are remarkably similar to those

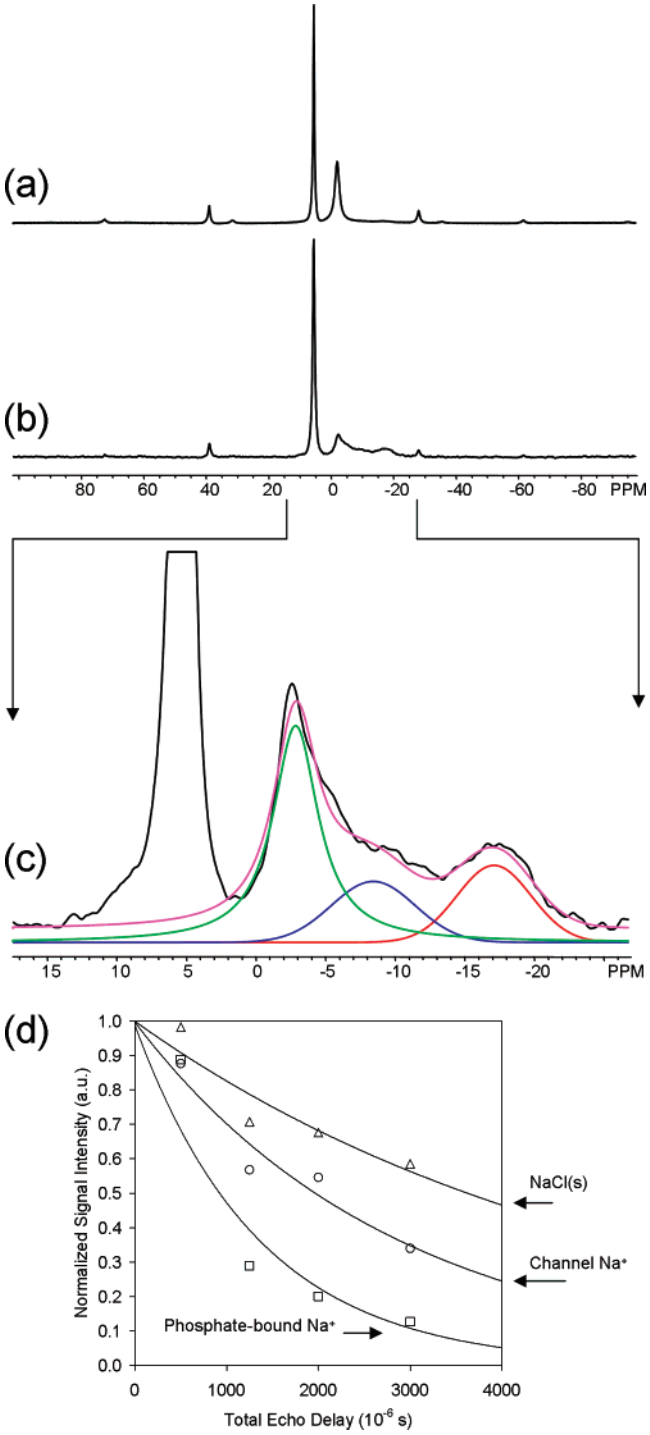

Figure 10. Solid-state ^{23}Na NMR spectra of d($G_4T_4G_4$) at 21.1 T. (a) Normal MAS spectra, (b,c) T_2-filtered MAS spectrum with a total spin−echo delay of 2.4 ms (sample spinning, 10 kHz), and (d) results from T_2 measurement for d($G_4T_4G_4$) at 11.75 T (sample spinning, 8 kHz). The T_2 values are 5.0 ms (NaCl), 2.8 ms (channel Na^+ ions), and 1.4 ms (phosphate-bound Na^+ ions).

(72) Samoson, A.; Kundla, E.; Lippmaa, E. *J. Magn. Reson.* **1982**, *49*, 350−357.

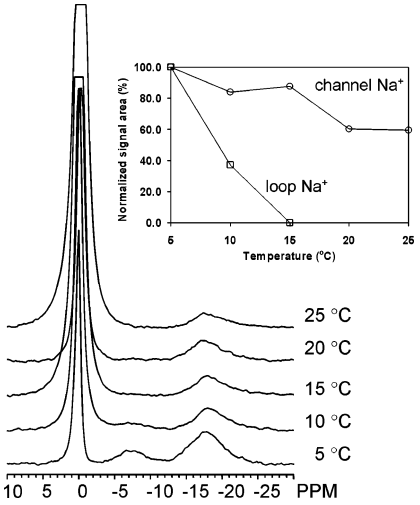

Figure 11. Variable-temperature ^{23}Na NMR spectra of d($G_4T_4G_4$) (5.4 mM strand concentration and $[Na^+]_{total} = 70$ mM). The interpulse delay was 5.3, 4.6, 4.0, 3.1, and 2.8 ms at 5, 10, 15, 20, and 25 °C, respectively. For each spectrum, approximately 800 000 transients were collected with a 20-ms recycle delay. Inset: Normalized ^{23}Na signal area as a function of temperature for loop and channel Na^+ ions. All spectra were obtained on a Bruker Avance-600 (14.1 T) spectrometer with temperature control to within 0.2 K.

obtained by Deng and Braunlin[41] from a three-site model analysis of the ^{23}Na NMR relaxation data for d($G_4T_4G_4$). It is possible that the bound Na^+ ions that Deng and Braunlin inferred in their relaxation data analysis correspond to the loop Na^+ ions. For the channel Na^+ ions, the fact that the ^{23}Na NMR line width shows very little temperature dependence suggests a much longer residence lifetime. In these conditions, the true channel Na^+ ions would contribute very little to the relaxation behavior of the free Na^+ ions. In this sense, the very slowly exchanging channel Na^+ ions in d($G_4T_4G_4$) are indeed "invisible" to the NMR relaxation methodology. On the basis of the recent experimental data reported by Plavec and co-workers[47] on a G-quadruplex containing mixed NH_4^+/Na^+ ions, we believe that the residence lifetime for the channel Na^+ ions in the pure Na^+ form of d($G_4T_4G_4$) should be on the order of several milliseconds, which is 2 orders of magnitude longer than that for the loop Na^+ ions.

K^+ Ions Compete for Both Loop and Channel Sites of d($G_4T_4G_4$). K^+ ions are known to have a higher binding affinity for the G-quadruplex channel site than Na^+ ions. Now that we have achieved spectral separation for the channel and loop Na^+ ions in d($G_4T_4G_4$), we decided to perform a K^+/Na^+ ion titration experiment to investigate Na^+ and K^+ binding affinity to these two different binding sites. Figure 12 shows the ^{23}Na NMR spectra of d($G_4T_4G_4$) in such an experiment. As expected, the signal intensity for the channel Na^+ ions decreases as the K^+ concentration is increased. This reflects the fact that, when K^+ ions are added to the DNA solution, they would replace the Na^+ ions already bound to the quadruplex channel sites. As also seen from Figure 12, when the K^+ concentration in the sample is increased, the ^{23}Na NMR signal for the loop Na^+ ions is also reduced at approximately the same rate as the channel signal. This observation suggests that the loop binding site also exhibits a higher affinity for K^+ ions than for Na^+ ions. Because the relative affinity between K^+ and Na^+ ions for the G-quadruplex channel site is known to be determined by a combination of the cation−carbonyl interaction energy and the cation dehydration energy,[55] it is reasonable to believe at this point that the Na^+ ion binding at the T_4 loop site should also involve coordination to carbonyl oxygen atoms and that the loop Na^+ ion must be significantly if not fully dehydrated. This picture is entirely consistent with the model shown in Figure 8.

Another consequence of having K^+ ions to replace the Na^+ ions already bound to the quadruplex at both channel and loop sites is that the ^{23}Na NMR relaxation behavior for the signal at $\delta = 0$ ppm is also changed. In particular, as the K^+ concentration is increased, the relaxation time for the free signal is lengthened considerably. For example, the T_1 value for the free Na^+ signal is changed from 12.0 ms without the added K^+ ions to 17.7 ms at 4.7 mM added K^+ concentration. As expected, once the loop sites are occupied by K^+ ions, the exchange process for Na^+ ions involves only the weakly bound (phosphate-bound) sites. In this aspect, our results are also consistent with the observation made by Braunlin and co-workers.[40,41]

Direct ^{23}Na NMR Evidence for a G-Quadruplex Channel Filled with Mixed Na^+ and K^+ Ions. Another striking feature seen in the spectra shown in Figure 12 is that, when K^+ is added to the Na^+ form of d($G_4T_4G_4$), a new ^{23}Na NMR signal appears at −15.7 ppm. This new signal can be assigned to the Na^+ ion residing inside the quadruplex channel but having a K^+ ion at the nearest binding site. As illustrated in Figure 12, we denote this new type of channel Na^+ ions as Type II. As expected, the relative population of this new signal increases with the K^+ concentration. In principle, there should also exist another type of Na^+ ions (Type III) which reside at the inner site with two K^+ ions occupying the two outer sites; however, the concentration for this type of Na^+ ions would be extremely low in the samples we prepared, i.e., $[K^+] \ll [Na^+]$. In a recent study, we reported similar effects in ^{23}Na NMR spectra of 5′-GMP.[64] There are several previous studies where a G-quadruplex channel was found to contain mixed ions. For example, Caceres et al.[21] reported two crystal structures for d(TG_4T) where mixed Tl^+ and Na^+ ions occupy the quadruplex channel. Neidle and co-workers[25] also found mixed Ca^{2+} and Na^+ ions in the d(TG_4T) quadruplex. Sundaralingam and co-workers[19] found mixed Ba^{2+} and Na^+ ions in a RNA quadruplex formed by (^{Br}dU)r(GAGGU). Plavec and co-workers[48] reported ^{1}H NMR evidence for the presence of mixed NH_4^+ and K^+ (or Na^+) ions in d($G_3T_4G_4$). These previous studies were based on either X-ray crystallographic or solution ^{1}H and $^{15}NH_4^+$ NMR data. Here we demonstrate that solution ^{23}Na NMR can also yield this type of information in a straightforward fashion. More importantly, our results illustrate the remarkable sensitivity of the ^{23}Na NMR chemical shift to subtle difference in ion coordination environment.

A Hypothesis on Monovalent Cation Binding in Diagonal T_4 Loops. To generalize our discussion on ion binding in diagonal T_4 loop regions, we first turn our attention to a comparison between our model for loop Na^+ binding and the mode of K^+ binding in the same diagonal T_4 loop observed in the crystal structure of the K^+ form of d($G_4T_4G_4$) (PDB entry 1JPQ). As also shown in Figure 8, the loop K^+ ion is located above the terminal G-quartet plane, coordinating to four O6 atoms from the terminal G-quartet, two O2 atoms from the loop thymine bases (T5 and T7), and two water molecules in a square anti-prism geometry. A nearly identical loop K^+ ion was also

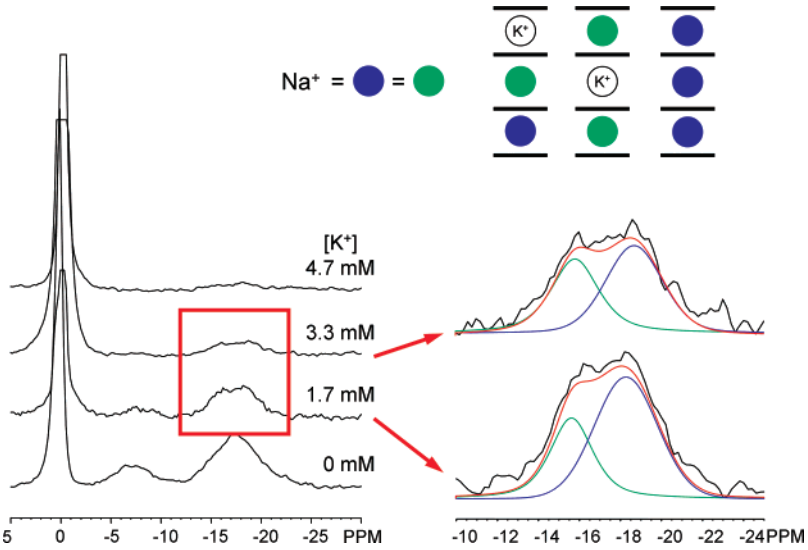

Figure 12. ^{23}Na NMR spectra of d($G_4T_4G_4$) from a K^+/Na^+ ion titration experiment. The interpulse delay was 8.3, 10.2, 12.0, and 12.8 ms for 0, 1.7, 3.3, and 4.7 mM K^+ ions, respectively. All ^{23}Na NMR spectra were recorded on a Bruker Avance-600 (11.7 T) spectrometer at 5 °C with 512 000 transients. Inset: Illustration of the Na^+ ion environment in a G-quadruplex channel containing mixed K^+ and Na^+ ions.

Table 2. Proposed Loop Cations and Corresponding Ligands in the First Coordination Sphere in the Diagonal T_4 Loop Region of Several DNA G-Quadruplexes

DNA	PDB entry	cation	ligands in the first coordination sphere
d($G_4T_4G_4$)	1K4X[56]	K^+	4 × O6(G) O2(T7), O2(T5) 2 × O_W (or a possible cation−π interaction)
d($G_4T_4G_4$)	2AKG[46]	Tl^+	4 × O6(G) O2(T7), O2(T5) 2 × O_W (or a possible cation−π interaction)
d($G_4T_4G_4$)	156D[67]	Na^+	4 × O6(G) O2(T7) O_W
d[G_4(TU)$_2G_4T_4G_4U_2T_2G_3$I]	230D[73]	Na^+	4 × O6(G) O2(T15) O_W
d[G_4(T_4G_4)$_3$]	201D[74]	Na^+	4 × O6(G) O2(T15), O2(T13)
d($G_3T_4G_3$)	1FQP[75]	Na^+	4 × O6(G) O2(T6), O2(T4)
d($G_4T_4G_3$)	1VLS[76]	Na^+	4 × O6(G) O2(T18), O2(T16)

observed in the crystal structure of a ligand−d($G_4T_4G_4$) complex (PDB entry 1L1H).[18] As expected, the K^+−O distances (K^+−O6, 3.00, 2.87, 2.88, and 3.08 Å; K^+−O2: 2.67 and 2.72 Å; K^+−O_W, 2.55 and 3.21 Å) are all considerably longer than the corresponding Na^+−O values. Another interesting feature in the crystal structure is that T5 and T7 bases form a wobble base pair, linked by a single O2(T5)···N3(T7) hydrogen bond. This hydrogen bond brings the T5 and T7 bases together so that the O2(T5) and O2(T7) atoms can coordinate to the K^+ ion simultaneously. In the NMR structure for the Na^+ form, however, the loop Na^+ ion can interact only with O2(T7), because the distance between the loop Na^+ ion and O2(T5) is too far (3.96 Å). From the loop ion point of view, the diagonal T_4 loop acts like a bidentate ligand for the larger K^+ ion but only a monodentate ligand for the Na^+ ion. This discrepancy in ligand binding mode may further enhance the preference of the loop binding site in d($G_4T_4G_4$) for K^+ over Na^+, in addition to the dehydration consideration mentioned earlier.

The above comparison also yields a plausible explanation for the different T_4 loop structures observed for the different ionic forms of d($G_4T_4G_4$). When the loop site is occupied by a Na^+ ion, the loop Na^+ ion is only coordinated to O2(T7). When a larger cation such K^+ or Tl^+ enters the loop region, it is coordinated to both O2(T7) and O2(T5). Thus, the loop structure is more compact and less flexible in the K^+ and Tl^+ forms of d($G_4T_4G_4$) than in the Na^+ form. This hypothesis is supported by the NMR structures of the K^+ and Tl^+ forms of d($G_4T_4G_4$) (PDB entries 1K4X[56] and 2AKG[46]), where O2(T7) and O2(T5) indeed point to the pocket above the terminal G-quartet, potentially available for ion binding.

We have further examined a total of seven known NMR structures for G-quadruplexes containing diagonal T_4 loops. As seen from Table 2, three structures are for different ionic forms of d($G_4T_4G_4$). Two are related to another *Oxytricha* telomere sequence, d($G_4T_4G_4T_4G_4T_4G_4$), each of which forms a unimolecular G-quadruplex containing two lateral T_4 loops and one diagonal T_4 loop (T13−T14−T15−T16).[73,74] In the presence of Na^+ ions, d($G_3T_4G_3$) forms an asymmetric bimolecular G-quadruplex containing two diagonal T_4 loops.[75] The NMR structure of d($G_4T_4G_3$) shows a similar asymmetric bimolecular

(73) Smith, F. W.; Schultze, P.; Feigon, J. *Structure* **1995**, *3*, 997−1008.
(74) Wang, Y.; Patel, D. J. *J. Mol. Biol.* **1995**, *251*, 76−94.

fold-back quadruplex but with two different T_4 loops.[76] One T_4 loop (T16−T17−T18−T19) spans diagonally across a terminal G-quartet, and the other T_4 loop (T5−T6−T7−T8) is entangled with two guanine bases (G4 and G12) not involved in G-quartet formation. Interestingly, all diagonal T_4 loop structures exhibit the following common features. First, there exists a cavity between the T_4 loop and the terminal G-quartet surrounded by electron-rich (partially negative) carbonyl groups. Second, the third thymine base along the strand direction (5′→3′) is always stacked on a nonsequential guanine base from the opposite diagonal, so that the O2 atom of this thymine forms a boundary of the central pocket. Third, the first thymine has its O2 atom either in the vicinity of or directly pointing toward the central pocket. These well-conserved structural features for a diagonal T_4 loop, coupled with the new ^{23}Na NMR results presented in this study, have led us to hypothesize that monovalent cations (Na^+, K^+, and Tl^+) are generally present in all diagonal T_4 loops. As summarized in Table 2, we further hypothesize that the loop Na^+ ion requires a hexa-coordination environment and that the larger ions such as K^+ and Tl^+ occupy the loop binding site in an octa-coordination geometry. This hypothesis seems to be consistent with all experimental ^{1}H, ^{23}Na, and ^{205}Tl NMR and crystallographic data. Meanwhile, the case of the NH_4^+ form of d($G_4T_4G_4$) remains to be a puzzle, because Feigon and co-workers[43] and, more recently, Plavec and co-workers[47] did not find any evidence for a NH_4^+ ion to reside in the diagonal T_4 loop region.

The last two cases shown in Table 2 deserve further discussion. For d($G_3T_4G_3$) and d($G_4T_4G_3$), Na^+ ions promote the formation of a bimolecular fold-back quadruplex structure, but K^+ and NH_4^+ ions tend to unfold the hairpin quadruplex structure into a linear quadruplex structure.[76,77] Clearly, the effect of K^+ and NH_4^+ ions in these two particular cases is to unwind (or at least destabilize) the T_4 loop of a fold-back quadruplex structure. The NMR structures of these two G-quadruplexes (PDB entries 1FQP[75] and 1VLS[76]) indicate that, in the presence of Na^+ ions, the third and first thymine bases, T6, T4 in d($G_3T_4G_3$) and T18, T16 in d($G_4T_4G_3$), are linked by the same O2(T)···N3(T) hydrogen bond as observed in the crystal structure for the K^+ form of d($G_4T_4G_4$). Therefore, the loop Na^+ ion should be coordinated to four O6 atoms from the end G-quartet and two O2(T) atoms. When a larger K^+ (or NH_4^+) ion enters the T_4 loop region, it would push back the two O2-(T) atoms, because a K^+−O coordination requires a longer K^+−O separation than a Na^+−O coordination. The consequence may be a breakdown of the O2(T)···N3(T) hydrogen bond, which in turn would destabilize the T_4 loop. Although it is unclear to what extent the loop ion binding contributes to the overall T_4 loop stability, the above rationale appears to provide a new compelling explanation for the observed cation effect in d($G_3T_4G_3$) and d($G_4T_4G_3$). Because it is still a challenging task to use the currently available molecular dynamics simulation methodologies to predict the loop structures in G-quadruplex DNA,[78] the new information presented in this study indicate that the inclusion of a proper monovalent cation in the T_4 loop region is important.

Conclusions

We have demonstrated a new multinuclear NMR approach for studying alkali metal ion binding to G-quadruplex DNA. We have shown that Na^+ and Rb^+ ions residing inside G-quadruplex channel are "NMR visible" in solution. We have directly measured the competitive Rb^+ and Na^+ binding to the G-quadruplex channel site. This represents the first time that competitive ion binding to a particular site in DNA can be *directly* monitored by simultaneous NMR detection of the two competing metal ions. We have found strong evidence for Na^+ ion binding to the diagonal T_4 loop of the G-quadruplex formed by d($G_4T_4G_4$). The residence lifetime for the Na^+ ions bound to the T_4 loop site is estimated to be 220 μs at 15 °C, which is 2 orders of magnitude shorter than that of the Na^+ ions bound to the G-quadruplex channel site. Our hypothesis is that monovalent cation binding to the diagonal T_4 loop of a G-quadruplex may be a general phenomenon. The reported high spectral resolution for G-quadruplex DNA is unprecedented in solution ^{23}Na NMR studies for biological macromolecules. We have also demonstrated that *ab initio* ^{23}Na chemical shift calculations can provide a link between experimental results and ion coordination geometry. Our results strongly suggest that solution multinuclear NMR of alkali metals is a viable technique for studying alkali metal ion binding to DNA. A combination of solution, solid-state NMR experimental methodologies, and quantum chemical calculation constitutes a general approach that can yield a wealth of information about ion binding in G-quadruplex DNA. Furthermore, we anticipate that a similar NMR approach can be applied to study ion binding to other biological systems, such as ion channel proteins.

Acknowledgment. This work was supported by the Natural Sciences and Engineering Research Council (NSERC) of Canada. R.I. thanks Queen's University for an R. S. McLaughlin Fellowship (2005−2006) and a Graduate Dean's Doctoral Field Travel Grant (2006). Access to the 900 MHz NMR spectrometer was provided by the National Ultrahigh Field NMR Facility for Solids (Ottawa, Canada), a national research facility funded by the Canada Foundation for Innovation, the Ontario Innovation Trust, Recherche Québec, the National Research Council Canada, and Bruker BioSpin and managed by the University of Ottawa (www.nmr900.ca). NSERC of Canada is acknowledged for a Major Resources Support grant. We also thank Dr. Victor Terskikh for technical assistance.

Supporting Information Available: Complete ref 60. This material is available free of charge via the Internet at http://pubs.acs.org.

JA709975Z

(75) Keniry, M. A.; Strahan, G. D.; Owen, E. A.; Shafer, R. H. *Eur. J. Biochem.* **1995**, *233*, 631−643.
(76) Crnugelj, M.; Hud, N. V.; Plavec, J. *J. Mol. Biol.* **2002**, *320*, 911−924.
(77) Strahan, G. D.; Keniry, M. A.; Shafer, R. H. *Biophys. J.* **1998**, *75*, 968−981.
(78) Fadrna, E.; Spackova, N.; Stefl, R.; Koca, J.; Cheatham, T. E., III; Sponer, J. *Biophys. J.* **2004**, *87*, 227−242.